Rhinology, 46, 213-220, 2008

Ventilation and drug delivery to the paranasal sinuses: studies in a nasal cast using pulsating airflow*

Winfried Möller[1], Uwe Schuschnig[2], Gabriele Meyer[3], Heribert Mentzel[2], Manfred Keller[2]

[1] Clinical Cooperation Group, Inflammatory Lung Diseases', Helmholtz Center Munich - German Research Center for Environmental Health, Gauting, Germany
[2] Pari GmbH, Munich and Starnberg, Germany
[3] Department of Nuclear Medicine, Asklepios Hospital Munich-Gauting, Gauting, Germany

SUMMARY

Background: *Although there is a high incidence of nasal disorders including chronic sinusitis, there is limited success in the topical drug delivery to the nose and the paranasal sinuses. This is caused by the nose being an efficient filter for inhaled aerosol particles and the paranasal sinuses being virtually non ventilated*

Method: *The objective of this study was to visualize the efficiency of sinus ventilation in a nasal cast using dynamic ^{81m}Kr-gas imaging in combination with pulsating airflows. Furthermore, the efficiency of the deposition of radiolabelled aerosol was assessed.*

Results: *Pulsation increased ventilation efficiency of the sinuses more than fivefold and aerosol deposition efficiency more than twentyfold, compared to delivery without pulsation. Furthermore pulsation increased aerosol deposition in the nasal airways by a factor of three. Using pulsating airflow Kr-gas ventilation and aerosol deposition efficiencies increased with increasing sinus volume. Pulsating airflow resulted in a deposition of up to 8% of the nebulized drug within the sinuses compared to 0.2% without pulsation.*

Conclusions: *The study demonstrates the high efficiency of a pulsating airflow in paranasal sinus ventilation and aerosolized drug delivery. This proves that topical drug delivery to the paranasal sinuses in relevant quantities is possible.*

Key words: sinus ventilation, pulsating aerosol, krypton gas inhalation, scintigraphy, pari sinus

INTRODUCTION

Chronic sinusitis is one of the most commonly diagnosed chronic illnesses, and approximately 10 - 15 % of the European and US population suffer from chronic rhinosinusitis [1-3]. It is thought that inflammation of the nasal mucosa (i.e., rhinitis), due to bacterial or viral infections, allergies, or exposure to inhaled irritants, leads to acute sinusitis. Chronic inflammation of the nasal mucosa results in mucosal swelling, increased mucus secretion, loss of cilia, airway obstruction and blocked sinus drainage. Under these conditions, bacteria and viruses that are normally removed from the nasal cavity and sinuses by drainage of secretions may proliferate. This blockage of mucus drainage from the sinuses and reduced ventilation creates an environment for chronic rhinosinusitis [3-5]. Impaired mucociliary clearance in patients with primary ciliary dyskinesia may also cause chronic sinusitis [6-8].

The paranasal sinuses are air-filled cavities in the bones of the skull surrounding the nose, ranging in volume between 5 ml and 30 ml [9]. They communicate with the nose via narrow ducts – the ostia – of about 1 - 3 mm diameter and about 10 – 15 mm length [9,10]. Despite the fact that the sinuses are poorly-ventilated hollow organs, in vivo and in vitro studies have shown that nebulized drugs can be deposited into the paranasal sinuses, although at very low concentrations [11-16]. Therefore the primary option of treatment of chronic rhinosinusitis is surgery, often in combination with topical and systemic medical treatment [3,17].

Two physical mechanisms affect the transport of gas and aerosols into non-actively ventilated areas: diffusion and flow induction by pressure difference [15,18,19]. Flow induction by a pressure gradient has been found to be the most important factor for carrying particles into non-ventilated areas. Pulsating air flows or humming can be used to generate such pressure gradients. In spite of the widespread use of aerosols in respiratory diseases, only a few studies have been performed to assess ventilation and aerosol deposition into the paranasal sinuses [12,15].

*Received for publication: January 22, 2008; accepted: May 15, 2008

In a previous study we showed the efficiency of Kr-gas ventilation to the paranasal sinuses in a human volunteer using pulsating airflows [20], but no data on aerosol drug delivery are available.

The objective of this study was to systematically investigate sinus ventilation in a nasal cast using dynamic ^{81m}Kr-gas imaging in combination with pulsating airflows. Furthermore the deposition efficiency of radiolabelled aerosol was assessed using different configurations of ostia diameters and sinus volumes, in order to find optimal conditions for sinus ventilation and aerosol drug delivery. This may open the possibility of topical aerosol treatment of nasal and sinus disorders, such as rhinosinusitis.

MATERIALS AND METHODS

Nasal cast

To simulate the upper extrathoracic airways a nasal cast made of Polyoxymethylene (POM, Figure 1) was used. The sinuses were modeled by cylindrical glass vials of 5, 10 and 20 ml volumes, which reflect the volume of sinuses in man [21]. The ostia were inserts into the glass vial openings with opening diameters of 1, 2, 3 and 5 mm and 10 mm length, respectively. The vials with inserted ostia were attached to the nasal airways in order to model the right maxillary (MR), right frontal (FR), left frontal (FL) and left maxillary (ML) sinuses. The different configurations of ostia diameter and sinus volumes are shown in Table 1. The cast had a left and a right nostril and the inner airways were divided by a nasal septum with a connecting hole at the posterior end. The cast had no further channel to the throat. This configuration was chosen to represent ventilation of the nose while closing the soft palate, which prevents gas or aerosol delivery to the lung.

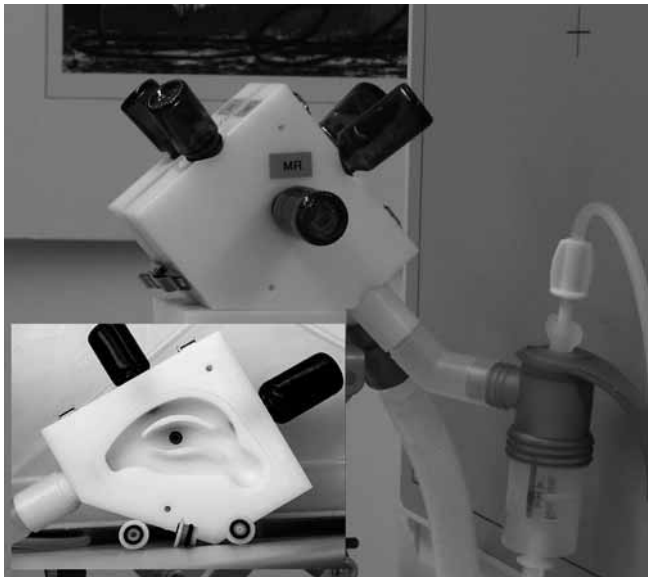

Figure 1. PARI nasal cast in front of the gamma camera including the nebulizer attached to the right nostril. Because of the overlap in the gamma camera imaging only the frontal and maxillary sinuses were active. The inset shows the right hemisphere of the PARI nasal cast, including right nostril, right sinuses and some sample ostia with different diameters in front of the cast.

Table 1. Configurations of ostium diameters between 1 mm (O1mm) and 5 mm (O5mm) and sinus volumes between 5 ml (S5ml) and 20 ml (S20ml) for right maxillary (MR), right frontal (FR), left frontal (FL) and left maxillary (ML) sinuses used to study Kr-gas ventilation and aerosol deposition in the nasal cast.

No.	MR	FR	FL	ML
#1	O1mm-S10ml	O1mm-S10ml	O1mm-S10ml	O1mm-S10ml
#2	O1mm-S5ml	O2mm-S5ml	O3mm-S5ml	O5mm-S5ml
#3	O1mm-S10ml	O2mm-S10ml	O3mm-S10ml	O5mm-S10ml
#4	O1mm-S20ml	O2mm-S20ml	O3mm-S20ml	O5mm-S20ml

Pulsating aerosol delivery system

A pulsating aerosol was generated using the PARI SINUS system. It is based on a PARI BOY N (PRONEB Ultra in the USA) aerosol drug delivery device. The compressor has an integrated pressure wave generator driven by the same motor. The pressure wave had 45 Hz frequency with an amplitude of 25 mbar (measured with a pressure transducer inside the model). It was attached via a tubing connector to the vent opening of a PARI LC SPRINT Junior jet nebulizer in order to superimpose the pressure wave on the aerosol flow. The mass median aerodynamic diameter (MMAD) of the aerosol generated by the PARI LC SPRINT Junior jet nebulizer was 3.2 μm with a geometric standard deviation of 2.6. The rate of mass output was 0.2 ml/min, and there was no difference in output rate with or without pulsation.

Kr-gas ventilation studies

^{81m}Kr-gas was continuously ventilated through the nasal cast in front of a single-head gamma camera (DIACAM, Siemens, Erlangen, Germany), using the PARI SINUS pulsating drug delivery system. The nebulizer was coupled to the right nostril and the left nostril was coupled via a flow resistor to output tubing, simulating the flow resistance of the human nose. The air supply of the PARI SINUS was directly taken from the ^{81m}Kr-gas generator output channel. The head of the gamma camera was equipped with a medium-energy collimator. Kr-gas ventilation imaging was performed with and without pulsation (Figure 2A and 2B). Serial images (2 frames per second, 30 seconds recording time) were recorded from the anterior view. This allowed dynamic studies of filling and emptying of the cast including the sinuses. Ventilation efficiency was studied for different ostium diameters and sinus volumes, as listed in Table 1. The gamma camera images were analyzed using the ImageJ 1.30 software package (http://rsb.info.nih.gov/ij/). For analysis of the distribution of the Kr-gas to the different compartments all serial images were superimposed (Figure 2). Regions of interest (ROI) of the nasal airways and the sinuses were defined as shown in Figure 2B and the activity was obtained in these ROI's. For background activity correction serial images were recorded without Kr-gas delivery.

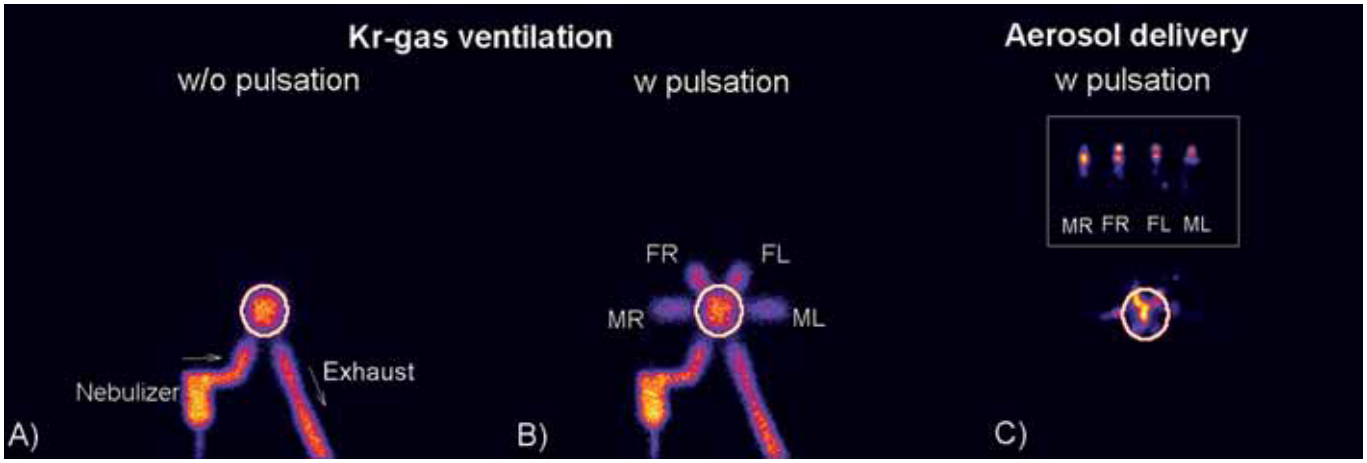

Figure 2. Anterior gamma camera images of Kr-gas ventilation of the nasal cast (configuration #1) without (w/o) pulsation (A) and with (w) pulsation (B). In addition the delivery system including the nebulizer connected to the right nostril is shown, as well as the exhaust tubing from the left nostril. C) Aerosol distribution in the cast after 2 min ventilation of a ^{99m}Tc-DTPA aerosol. The inset shows the separate arrangement of the four sinuses without the nasal airways.

Sinus aerosol targeting

An aerosol was generated using a solution composed of ^{99m}Tc-DTPA mixed 1:1 with 10 mg/ml disodium chromoglycate (DSCG) isotonic solution (Pari IsoCROM). This allows radioactive and chemical analysis of aerosol deposition in the various compartments of the nasal cast. The nebulizer was coupled to the right nostril and the left nostril was coupled via a flow resistor to an output filter. Prior to aerosol delivery to the nasal cast the output rate of the nebulizer was measured (with pulsation) by collecting all particles on a PALL BB50 filter (Pall Corporation, New York, NY, USA). Four milliliters of solution containing about 600 MBq of ^{99m}Tc-activity were added to the nebulizer. During a 2 minute running period the activity was detected by gamma camera imaging. For aerosol targeting to the nasal cast the nebulizer was coupled to the right nostril, while a PALL filter was coupled to the left nostril. This allowed measuring of the total deposition rate in the nasal cast.

The deposition efficiency was assessed for different ostium diameters and sinus volumes as shown in Table 1. After two minutes of aerosol delivery to each configuration, gamma camera images were recorded, as shown in Figure 2C. The activity deposition in the nasal cast and the sinuses (including ostia) was obtained using the ROI's defined during Kr-gas ventilation imaging. Additionally, images were obtained of the ostia-sinuses only and of the nasal airways only. Then the next configuration of ostia and sinuses was coupled to the airway model and the 2 minutes of aerosol delivery was repeated. At the end the total activity of the nasal airways and the activity left in the nebulizer were analyzed.

Besides the radioactive analysis using gamma camera imaging, chemical analysis of the amount of DSCG was assessed using a liquid chromatography system, equipped with a Waters PDA 996 detector. The calibration ranged from 1.0 to 150 μg/ml DSCG and was performed in two concentration ranges.

Data analysis

All studies were performed at least three times and mean values and standard deviations (SD) were calculated. Group differences were calculated by a two-sided t-Test (Winstat software package for Microsoft Excel, Version 2005.1, www.winstat.com), using a significance level of $p < 0.05$. Pearson correlation analysis was performed to analyze correlations between parameters.

RESULTS

Kr-gas ventilation of the nasal cast

Kr-gas ventilation images obtained with (w) and without (w/o) pulsation are shown in Figure 2. Figure 2A represents ventilation without pulsation. Only the central nasal airways appear on the image (bold ROI). In addition the delivery system is shown with the nebulizer (right nostril), as well as the exhaust tubing (left nostril). The sinuses do not appear on this image, suggesting that there is very little ventilation and Kr-gas penetration to the sinuses. Figure 2B illustrates the Kr-gas activity distribution w pulsation, where in contrast to Figure 2A the sinuses clearly display. This image was used to assess ROI's of all four sinuses (not shown). In this setup (#1) all four sinuses have equal volume (10 ml) and equal ostium diameter (1 mm). The activity distribution in the sinuses normalized to the total activity in the nasal cast (airways and sinuses) is illustrated in Figure 3. Activities in the delivery and exhaust system were not analyzed. Relative to the total activity in the nasal cast model, the activity was equally distributed to each of the four sinuses ranging between 12 and 13 %. Figure 3B shows the cumulative activity distribution to all the sinuses. With pulsation, the four sinuses contained 53 ± 3 % of Kr-gas activity of the whole nasal cast. Without pulsation, 8.7 ± 2.4 % of the total

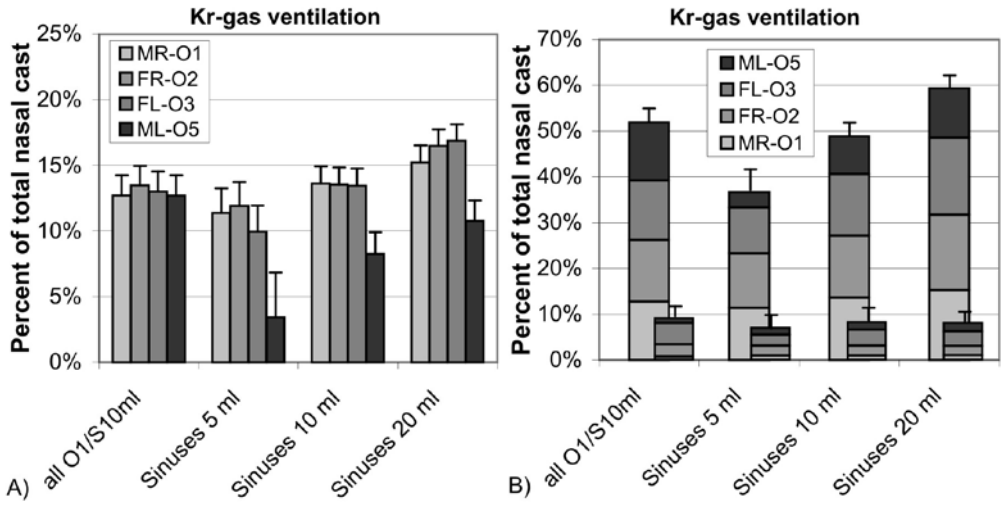

Figure 3. A) Kr-gas ventilation to the sinuses (percentage of activity in the whole nasal cast) with pulsation of the four different configurations of ostia diameter and sinus volume, as shown in Table 1. B) Cumulative ventilation efficiency in the different ostium/sinus configurations with pulsation. The superior bars show the cumulative ventilation efficiency of the sinuses without pulsation. Data show mean +/- SD (n=3).

activity within the nasal cast penetrated to the four sinuses ($p < 0.01$, Figure 3B, superior bars). Looking at results of the other three ostium/sinus configurations, it is evident that the fraction of activity penetrating to the sinuses depends on the sinus volume, with an increase from 36.7 ± 4.7 % to 59.4 ± 2.7 % of activity in the nasal cast for 5 ml and 20 ml sinuses, respectively ($p < 0.01$, Figure 3B). In addition the ostium openings play a significant role, where the largest ostium with 5 mm diameter shows the worst ventilation performance. Only the largest sinus volume gave reasonable ventilation in combination with the 5 mm ostium opening. The highest sinus ventilation was obtained using 2 and 3 mm ostium openings, independent of the sinus volume.

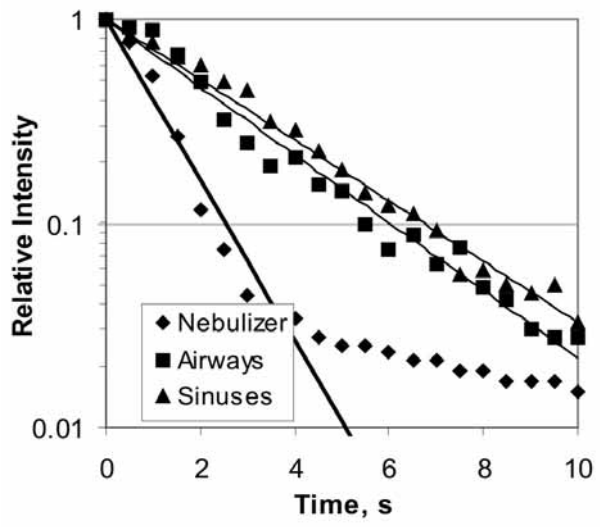

Figure 4. Wash out of the activity from the nebulizer, the nasal airways and the paranasal sinuses after switching off the Kr-gas delivery.

Figure 4 shows the wash out characteristics after switching off the Kr-gas delivery. The drop in activity for the nebulizer was much faster compared to that in the nasal airways or in the sinuses. In addition there was a delay in Kr-gas washout from the sinuses compared to the nasal airways.

Gamma camera imaging and chemical analysis

For analysis of aerosol penetration and subsequent deposition, the radioactive and the chemical DSCG analyses were applied similarly. For the radioactivity analysis the same ROI's as defined in the Kr-gas ventilation images were used. In addition, the bottles were removed from the cast and analyzed separately for radioactivity (see inset in Figure 2C). For chemical analysis the deposited aerosol was eluted from all compartments and analyzed for DSCG content. The DSCG content in each compartment showed a high linear correlation with the radioactivity count in each compartment (coefficient of correlation, $R = 0.99$, data not shown). Therefore the radioactivity analysis provided a reliable measure of the amount of deposited aerosol in each compartment.

Aerosol deposition in the nasal sinuses

Figure 2C illustrates the aerosol deposition in the nasal airways and in the sinuses (including ostia) with pulsating airflow for the first set of equal ostium openings and sinus volumes (#1, 1 mm ostium diameter and 10 ml sinus volume). The activity distribution was very nonhomogeneous and showed hot spots of deposition, in the nasal airways as well as in the sinuses, and high deposition fractions occurred at the ostia (see inset of Figure 2C).

Figure 5 shows the aerosol deposition distribution in the nasal airways and in the four sinuses of the different ostium/sinus configurations in relation to the activity deposited in the whole

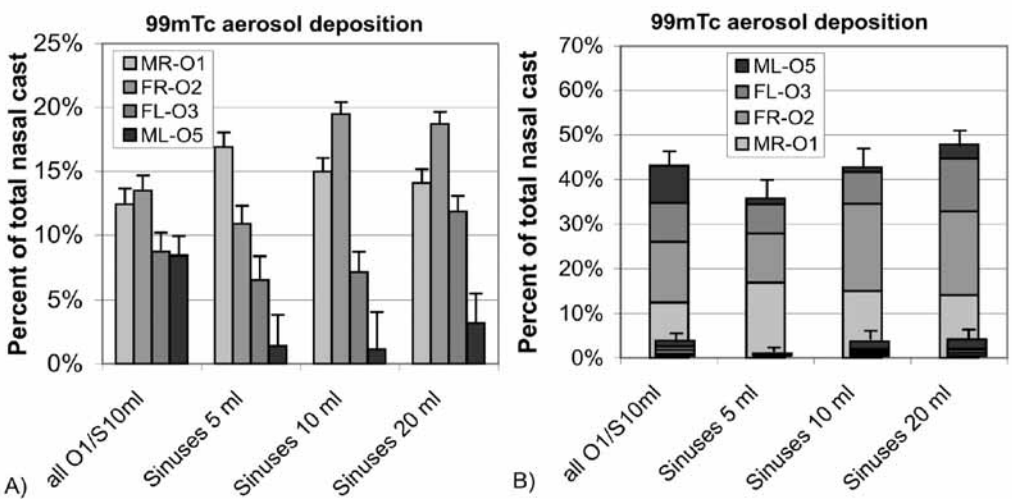

Figure 5. A) ^{99m}Tc aerosol deposition in the nasal sinuses in relation to the total drug deposited in the nasal cast (airways and sinuses) with pulsation for the four different configurations of ostium diameter and sinus volume, as shown in Table 1. B) Cumulative aerosol deposition efficiency in the different ostium/sinus configurations with pulsation. The superior bars show the cumulative deposition efficiency of the sinuses without pulsation. Data show mean +/- SD (n=3).

nasal cast (sinuses and airways). In the configuration with equal ostia and sinuses (#1, 1 mm ostium diameter and 10 ml sinus volume) the deposited activity was less homogeneously distributed between sinuses, compared to Kr-gas ventilation (Figure 3). The right sinuses (MR and FR) showed higher aerosol deposition (13.0 ± 1.0 %) compared to the left sinuses (FL and ML, 8.5 ± 0.5 %, $p < 0.01$), but there were no systematic differences between frontal and maxillary sinuses. This seems to reflect aerosol deposition in the right nasal airways and aerosol losses when passing from the right into the left nasal airway compartment. Studies performed after an interchange of the nebulizer to the left nostril and the exhaust filter to the right nostril confirmed this hypothesis with a higher aerosol deposition in the left sinuses.

The aerosol deposition pattern of the other three ostium-sinus configurations showed very specific characteristics (Figure 5). The 5 mm ostium diameter yielded the worst deposition efficiency in combination with all sinus volumes. For the 5 ml sinus volume there was a significant decrease of aerosol deposition with increasing ostium diameter. Aerosol deposition decreased from 16.9 ± 1.9 % for the 1 mm ostium diameter to 1.4 ± 2.4 % for the 5 mm ostium diameter. The 10 ml and 20 ml sinuses showed comparable characteristics in deposition distribution with a maximum of greater than 15 % deposition for the 2 mm ostium diameter. Deposition efficiencies increased for the 3 mm and 5 mm ostium openings with increasing sinus volume. This characteristic aerosol deposition distribution did not change when the nebulizer was connected to the left nostril. However the sinuses of the left airway hemisphere received a higher dose (as compared to nebulizer attachment to the right nostril). Figure 5B shows the cumulative aerosol deposition in relation to the total cast aerosol deposition of the different configurations. With pulsation total deposition in the four sinuses increased from 35.8 ± 3.5 % using the 5 ml sinuses to 47.9 ± 3.0% using the 20 ml sinuses ($p < 0.01$). Kr-gas sinus ventilation efficiencies and aerosol deposition efficiencies showed a significant correlation ($R = 0.73$, $p < 0.01$). The superior bars in Figure 5B show the ostium/sinus deposition efficiencies without pulsation. There was an increase in cumulative ostium/sinus deposition from 0.5 ± 0.8 % for the 5 ml sinuses to 3.7 ± 1.5 % for the 20 ml sinuses ($p < 0.01$). Contrary to the data with pulsation the sinuses with 5 mm ostium diameter got the highest activity without pulsation.

Figure 6A shows the deposition efficiency with pulsation in the different ostium-sinus configurations in relation to the amount of nebulized drug. Here we present the results of the DSCG-analysis, which is similar to the ^{99m}Tc activity analysis. The pattern was similar to the percentage of total nasal cast deposition distribution presented in Figure 5B. For optimal ostium diameter and sinus volume up to 3.5 ± 0.3 % of the nebulized drug was recovered in a sinus cavity. The aerosol deposition in the nasal airways during each 2 min aerosol ventilation was 8.1 ± 0.4% of the nebulized drug, independent of the ostium/sinus configuration, as shown in Figure 6B. The total deposition in all four sinuses in relation to the nebulized drug increased with sinus volume from 4.1 ± 0.3% using the 5 ml sinuses to 7.5 ± 0.4% using the 20 ml sinuses ($p < 0.01$).

The superior bars in Figure 6B show the deposition efficiencies in the nasal airways and in all four sinuses without pulsation. Deposition in the nasal airways decreased from 8.1 ± 0.4% with pulsation to 2.2 ± 0.2% without pulsation ($p < 0.01$). Without pulsation deposition in the sinuses increased from 0.02 ± 0.02% for the 5 ml sinuses to 0.18 ± 0.09 % of the nebulized drug for the 20 ml sinuses ($p < 0.01$).

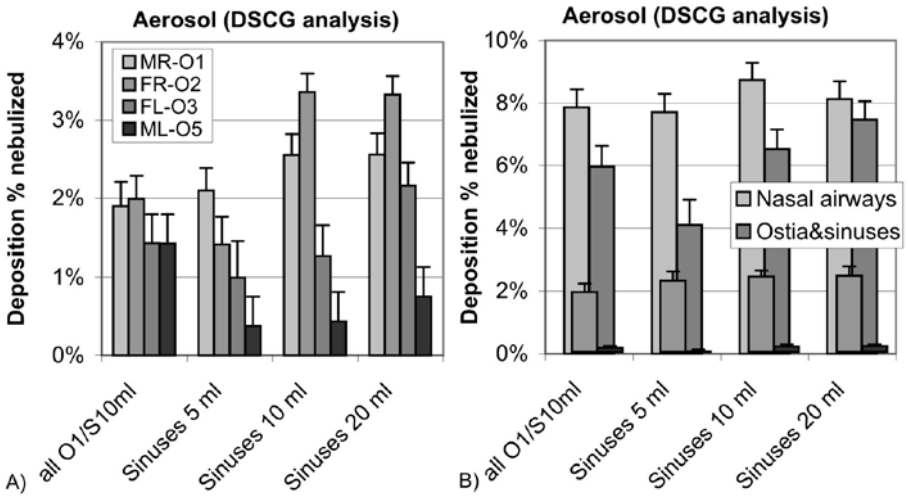

Figure 6. A) Aerosol deposition in the sinuses in relation to the nebulized aerosol of the four different configurations of ostium diameter and sinus volume (w pulsation). B) Aerosol deposition in the nasal airways and in the sinuses (cumulative) in relation to the nebulized aerosol of the four different experimental configurations (w pulsation). The superior bars show the respective aerosol deposition without pulsation. Data show mean +/- SD (n=3).

DISCUSSION

The inefficiency of ventilation of the paranasal sinuses using standard inhalation devices has been demonstrated by the 133-xenon washout technique [22,23]. Typical gas exchange half times are 10 to 30 min in healthy subjects, and further increased in patients with sinus diseases. This is not sufficient to transport significant amounts of drugs into the paranasal sinuses in order to perform a topical therapy. This efficiency can be significantly enhanced using pulsating airflow.

Kr-gas sinus ventilation

The efficiency of pulsating airflow for proper sinus ventilation is evident from Figure 2. Without pulsation, less than 10 % of the total Kr-gas activity within the nasal cast penetrated to the sinuses. This rate increased to about 50 % with pulsation. This demonstrates that generation of significant pressure differences at the ostium openings leads to increased transport of gas. Our study shows that there are optimal combinations of ostium diameter and sinus volume for maximal sinus ventilation with pulsation. The worst configuration appears to be that of the 5 mm ostium diameter, for all three sinus volumes used. Ostium openings of two or three millimeters may be most efficient for sinus ventilation in conjunction with pulsating airflow. These optimum conditions of ventilation of the sinuses may reflect a resonance behavior, since the ostia and sinuses can be considered as a Helmholtz-resonator like configuration. However experimental and simulation investigations show resonance behavior with an efficient gas exchange for similar configurations of ostium diameter and sinus volume at higher pulsation frequencies of above 100 Hz, while our device operates at 45 Hz [9,15].

The sinuses caused a sustained release of activity from the nasal cast after switching off the radioactive gas delivery. As can be seen from Figure 4 the activity drop was much slower in the nasal airways compared to that in the nebulizer, and was further slowed in the sinus cavities. This indicates a delay in gas exchange between sinuses and nasal airways. This delay could cause an increased residence time of an aerosol drug in the sinuses and this could enhance the deposition fraction. Paranasal sinus washout without pulsation is much slower than with pulsation, as has been shown using ^{133}-Xenon scintigraphy [22].

Aerosol deposition

Aerosol deposition in the nasal airways increased from 2.2 ± 0.2% without pulsation to 8.1 ± 0.4 % with pulsation. Increased aerosol deposition in a cast and in the nose using pulsating airflow has been shown before by Sato et al. [11]. The difference in aerosol delivery with and without pulsation to the sinuses was much larger (factor $>$ 20) than was observed for the Kr-gas ventilation (factor 5-6). This result supports the significance of aerosol delivery and deposition using pulsating airflows.

In relation to the total aerosol deposition in the nasal cast the deposition in the right sinuses (FR and MR) was comparable to Kr-gas ventilation, while it was lower in the left sinuses (which was not seen in the Kr-gas ventilation study). Aerosol deposition in the right airway cavity and the passage from the right nasal cavity into the left cavity seems to cause losses in aerosol concentration. When the nebulizer was exchanged and coupled to the left nostril aerosol deposition in the left airway cavity was higher than in the right airway cavity (data not shown). However, this interchange did not alter the aerosol deposition pattern of the different ostium/sinus configurations. In order to compensate for this effect a correction by a factor of 1.5 for the left ostia/sinuses would be appropriate. This correction was not applied in our analysis because it does not alter

the specific deposition pattern. Optimal drug delivery to all sinuses would imply nebulization to both nostrils one after the other at equal durations.

The dependency of aerosol deposition on the combination of ostium diameter and sinus volume was more pronounced for aerosol deposition compared to Kr-gas ventilation. The ostium with 5 mm diameter showed the worst deposition efficiency. Using the small 5 ml sinus volume there was a strong decrease of aerosol deposition with increasing ostium diameter. This behavior was not seen for the larger sinuses. The 10 ml and 20 ml sinuses showed maximum deposition using the 2 mm ostium diameter. A similar maximum was not seen during Kr-gas ventilation. These data may imply a resonance effect between nasal ostium and sinus geometry, and pulsating airflow parameters. These data suggest, that for given anatomical conditions, pulsation parameters (frequency, amplitude) may be optimized for maximum penetration.

Although deposition is much lower without pulsation the sinuses with 5 mm ostium diameters got the highest dose compared to the smaller ostium diameters (more than 50 % of the dose deposited in all sinuses). The gamma camera images showed that most of this dose was deposited in the ostia. Although aerosol delivery to sinuses with larger ostium diameters is more efficient without pulsation, the total deposited drug is much lower compared to conditions with pulsation, as can be seen from Figures 5B and 6B.

Durand et al. [24] used a more realistic plastinated nasal cast of a human cadaver and measured aerosol deposition by gamma camera imaging, with and without sounding airflow. Using sounding airflow they could confirm activity penetration into the sinuses, but only just above the gamma camera background activity. They did not give any estimation on absolute deposition efficiencies in their study. Maniscalco et al. [15] could also show that sounding airflow (humming) causes an increase in sinus drug deposition in human volunteers, enhancing the delivery of a nitric oxide-synthase inhibitor to the nasal sinuses and thereby reducing the release of nasal NO during humming. Drug delivery without sounding airflow had no effect on nasal NO release.

Opportunities for the aerosol treatment of nasal disorders

Results from studies using a nasal cast model can only be partly applied to a real human nose, because most models lack anatomical nasal structures. In addition ventilation and aerosol deposition conditions may further change in the diseased nose. Nevertheless models are useful to understand the conditions of optimal nasal sinus ventilation and optimal aerosol deposition. The complex structure of the nasal airways causes high particle deposition at the nasal valve and the nasal turbinates, especially of larger particles. This makes the nose an efficient filter for inhaled pollutants. However, it also significantly reduces the amount of aerosol penetrating to areas where there is access to the sinus cavities. This is a limiting factor in most of the studies published in relation to aerosolized nasal or sinus drug delivery. Using our nasal cast model between 40 and 50 % of aerosol that deposited in the nasal cast was deposited into the sinuses, which relates to 4% - 8% deposition efficiency in all sinuses in relation to the nebulized drug (see Figure 6B). Although 8 % aerosol deposition in the nasal sinuses appears low, it may provide sufficient drug delivery for a topical inhalative aerosol therapy.

Patients with nasal airway obstructions, caused either by nasal polyps or by the inflamed mucosa, such as patients with chronic sinusitis, may benefit from aerosolized drug delivery using pulsating airflows [25]. However, a principal limitation of aerosol drug delivery to the sinuses is that ventilation has to be possible. Obstructed sinuses did not show enhanced NO release after humming, as was shown by Lundberg et al. [26]. Nevertheless these patients may benefit from pulsating aerosol delivery by an increased aerosol deposition in nasal airways.

In summary our model cast study showed that aerosol delivery to the sinuses was negligible without pulsation. Using pulsating airflow some percentage of the nebulized drug deposited in a sinus cavity. In addition pulsating airflow enhanced aerosol deposition in the nasal airways. This enhanced drug delivery may also improve aerosol treatment of other nasal disorders, such as impaired mucociliary clearance, rhinitis or bacterial infections.

REFERENCES

1. Van Cauwenberge P, Watelet JB. Epidemiology of chronic rhinosinusitis. Thorax 2000; 55: 20S-1.
2. MedlinePlus. Sinusitis Fact Sheet, January 2006. Washington, DC: National Institute of Allergy and Infectious Diseases; 2006 [updated 2006; cited]; Available from: http://www.niaid.nih.gov/factsheets/sinusitis.htm.
3. Fokkens W, Lund V, Mollol J et al. The European Position Paper on Rhinosinusitis and Nasal Polyps (EP3OS) group. Rhinology 2007; 45, Suppl. 20: 1-137.
4. Clement PA. Definitions of sinusitis. Acta Otorhinolaryngol Belg 1997; 51: 201-203.
5. Baraniuk J, Maibach H. Pathophysiological classification of chronic rhinosinusitis. Respir Res 2005; 6: 149.
6. Armengot M, Juan G, Barona R, Garin L, Basterra J. Immotile cilia syndrome: nasal mucociliary function and nasal ciliary abnormalities. Rhinology 1994; 32: 109-111.
7. Min YG, Shin JS, Choi SH, Chi JG, Yoon CJ. Primary ciliary dyskinesia: ultrastructural defects and clinical features. Rhinology 1995; 33: 189-193.
8. Noone PG, Leigh MW, Sannuti A, et al. Primary ciliary dyskinesia - Diagnostic and phenotypic features. Am J Respir Crit Care Med 2004; 169: 459-467.
9. Tarhan E, Coskun M, Cakmak O, Celik H, Cankurtaran M. Acoustic rhinometry in humans: accuracy of nasal passage area estimates, and ability to quantify paranasal sinus volume and ostium size. J Appl Physiol 2005; 99: 616-623.
10. Jones N. The nose and paranasal sinuses physiology and anatomy. Adv Drug Deliv Rev 2001; 51: 5-19.

11. Sato Y, Hyo N, Sato M, Takano H, Okuda S. Intra-nasal distribution of aerosols with or without vibration. Z Erkr Atmungsorgane 1981; 157: 276-280.
12. Hyo N, Takano H, Hyo Y. Particle deposition efficiency of therapeutic aerosols in the human maxillary sinus. Rhinology 1989; 27: 17-26.
13. Suman JD. Nasal drug delivery. Expert Opin Biol Th 2003; 3: 519-523.
14. Saijo R, Majima Y, Hyo N, Takano H. Particle deposition of therapeutic aerosols in the nose and paranasal sinuses after transnasal sinus surgery: a cast model study. Am J Rhinol 2004; 18: 1-7.
15. Maniscalco M, Sofia M, Weitzberg E, Lundberg JO. Sounding airflow enhances aerosol delivery into the paranasal sinuses. Eur J Clin Invest 2006; 36: 509-513.
16. Kimbell JS, Segal RA, Asgharian B, et al. Characterization of Deposition from Nasal Spray Devices Using A Computational Fluid Dynamics Model of The Human Nasal Passages. J Aerosol Med 2007; 20: 59-74.
17. Gosepath J, Mann WJ. Current Concepts in Therapy of Chronic Rhinosinusitis and Nasal Polyposis. ORL 2005; 67: 125-136.
18. Kauf H. Eindringvermögen von Aerosolen in Nebenräume [Penetration ability of aerosols into secondary spaces]. Eur Arch Otorhinolaryngol 1968; 190: 95-108.
19. Böhm A, Luber M, Mentzel H, Knoch M. Investigating Drug Delivery to the Sinuses: An In Vitro Deposition Study Using a Nasal Cast Model. Respiratory Drug Delivery IX 2004; 3: 601-604.
20. Möller W, Schuschnig U, Meyer G, et al. Visualization of human sinus ventilation by radioactive Krypton using the Pari Sinus pulsating system. In: Dalby RN, Byron PR, Peart J, Suman JD, editors. Respiratory Drug Delivery Europe 2007. Paris, France: Virginia Commonwealth University. 2007. p275-278.
21. Sánchez Fernández JM, Anta Escuredo JA, Sánchez Del Rey A, Santaolalla Montoya F. Morphometric study of the paranasal sinuses in normal and pathological conditions. Acta Otolaryngol (Stockh) 2000; 120: 273-278.
22. Paulsson B, Dolata J, Larsson I, Ohlin P, Lindberg S. Paranasal sinus ventilation in healthy subjects and in patients with sinus disease evaluated with the 133-xenon washout technique. Ann Otol Rhinol Laryngol 2001; 110: 667-674.
23. Paulsson B, Lindberg S, Ohlin P. Washout of 133-xenon as an objective assessment of paranasal sinus ventilation in endoscopic sinus surgery. Ann Otol Rhinol Laryngol 2002; 111: 710-717.
24. Durand M, Rusch P, Granjon D, et al. Preliminary study of the deposition of aerosol in the maxillary sinuses using a plastinated model. J Aerosol Med 2001; 14: 83-93.
25. Knipping S, Holzhausen H, Riederer A, Bloching M. Cystic fibrosis: ultrastructural changes of nasal mucosa. Eur Arch Otorhinolaryngol 2007; 264: 1413-1418.
26. Lundberg JO, Maniscalo M, Sofia M, Lundblad L, Weitzberg E. Humming, Nitric Oxide, and Paranasal Sinus Obstruction. JAMA 2003; 289: 302-303.

Dr. Winfried Möller
Helmholtz Center Munich - German Research Center for Environmental Health
Clinical Cooperation Group 'Inflammatory Lung Diseases'
Robert-Koch-Allee 29
D-82131 Gauting
Germany

Tel: +49-89-3187 1881
Fax: +49-89-3187 191881
E-mail: moeller@helmholtz-muenchen.de